


Article

Spatial Heterogeneity and Complexity of the Impact of Extreme Climate on Vegetation in China

Shuang Li ^{1,2}, Feili Wei ^{1,2}, Zheng Wang ^{1,2}, Jiashu Shen ^{1,2}, Ze Liang ^{1,2} , Huan Wang ^{1,2} and Shuangcheng Li ^{1,2,*}

¹ College of Urban and Environmental Sciences, Peking University, Beijing 100871, China; chls@pku.edu.cn (S.L.); weifeili@pku.edu.cn (F.W.); wz1992@pku.edu.cn (Z.W.); jiashu_shen@pku.edu.cn (J.S.); liangze@pku.edu.cn (Z.L.); 2001111811@stu.pku.edu.cn (H.W.)

² Key Laboratory for Earth Surface Processes of the Ministry of Education, Peking University, Beijing 100871, China

* Correspondence: scli@urban.pku.edu.cn

Abstract: The impact of extreme climate on natural ecosystems and socioeconomic systems is more serious than that of the climate's mean state. Based on the data of 1698 meteorological stations in China from 2001 to 2018, this study calculated the 27 extreme climate indices of the Expert Team on Climate Change Detection and Indices (ETCCDI). Through correlation analysis and collinearity diagnostics, we selected two representative extreme temperature indices and three extreme precipitation indices. The spatial scale of the impact of extreme climate on Normalized Difference Vegetation Index (NDVI) in China during the growing season from 2001 to 2018 was quantitatively analyzed, and the complexity of the dominant factors in different regions was discussed via clustering analysis. The research results show that extreme climate indices have a scale effect on vegetation. There are spatial heterogeneities in the impacts of different extreme climate indices on vegetation, and these impacts varied between the local, regional and national scales. The relationship between the maximum length of a dry spell (CDD) and NDVI was the most spatially nonstationary, and mostly occurred on the local scale, while the effect of annual total precipitation when the daily precipitation amount was more than the 95th percentile (R95pTOT) showed the greatest spatial stability, and mainly manifested at the national scale. Under the current extreme climate conditions, extreme precipitation promotes vegetation growth, while the influence of extreme temperature is more complicated. As regards intensity and range, the impact of extreme climate on NDVI in China over the past 18 years can be categorized into five types: the humidity-promoting type, the cold-promoting and drought-inhibiting compound type, the drought-inhibiting type, the heat-promoting and drought-inhibiting compound type, and the heat-promoting and humidity-promoting compound type. Drought is the greatest threat to vegetation associated with extreme climate in China.

Keywords: extreme climate; vegetation; spatial heterogeneity; dominant factors



Citation: Li, S.; Wei, F.; Wang, Z.; Shen, J.; Liang, Z.; Wang, H.; Li, S. Spatial Heterogeneity and Complexity of the Impact of Extreme Climate on Vegetation in China. *Sustainability* **2021**, *13*, 5748. <https://doi.org/10.3390/su13105748>

Academic Editor: Jakub Brom

Received: 22 April 2021

Accepted: 17 May 2021

Published: 20 May 2021

Publisher's Note: MDPI stays neutral with regard to jurisdictional claims in published maps and institutional affiliations.



Copyright: © 2021 by the authors. Licensee MDPI, Basel, Switzerland. This article is an open access article distributed under the terms and conditions of the Creative Commons Attribution (CC BY) license (<https://creativecommons.org/licenses/by/4.0/>).

1. Introduction

Against the background of global climate change, all countries are seeking to comprehensively control greenhouse gas emissions and deal with climate warming. Compared with climate mean state change, extreme climate change has more aspects, greater amplitude, and causes more potential damage, posing a greater threat to the natural ecosystem and socioeconomic systems [1–5].

Vegetation is a common risk receptor in the study of climate change. It is also an extremely important carbon source and sink in terrestrial ecosystems, and plays an important role in the global carbon cycle. Studies have shown that in the past few decades, terrestrial ecosystems have absorbed large amounts of carbon dioxide emitted by human activities, and have effectively regulated the carbon cycle [6]. Studies have shown that compared with the climate mean state and the slow increment of climate change, ecosystem biodiversity is mainly affected by extreme climate change [7–10]. The response of vegetation to climate

change, especially extreme climate events, has also been acknowledged in many places around the world [11–13].

A series of vegetation indices are often used to characterize, analyze, and evaluate the activity of vegetation. Satellite-based data are based on algorithms that estimate the target variables; however, there are clear advantages. With the progress of science and technology, satellite-based data have overcome some of the limitations of field observation and research due to their characteristics of easy access, long time series, and large spatial scale, and they have been assigned great importance by academics. The Normalized Difference Vegetation Index (NDVI), obtained via remote sensing, is widely used in vegetation research, especially in the study of the relationship between climate factors and vegetation [14–19].

China is one of the countries most affected by extreme climate events and disasters. At the same time, China is rich in vegetation resources of various types and regional characteristics, and so is also commonly used for vegetation research. Recently, researchers have conducted statistical studies, model simulation studies and experimental observational studies, based on different data sources, of the effects of extreme climate change on vegetation in China, at a variety of spatial and temporal scales [20]. For example, some research was carried out in the Loess Plateau, which is an ecologically vulnerable region in China [21]. In addition, there is research focused on the typically agricultural areas of China to discuss the threats of drought and frost to the vegetation, which are important in the practice of actual agricultural production [22,23]. At present, the research is mainly focused on specific ecologically vulnerable or sensitive areas in China, and analysis on the national scale is relatively rare. Furthermore, the research mainly concentrates on the degree and direction of the influence, and the temporal hysteresis [24]. However, few studies deeply and quantitatively discuss the spatial heterogeneity of the impacts of different extreme climatic elements on vegetation. In addition, the regional complexity of the combined effects of extreme temperature and precipitation need to be considered thoroughly.

This study takes China as the focus to assess the impacts of extreme climate on vegetation, based on data from meteorological stations and NDVI. The main scientific questions to be addressed are as follows: (1) what are the effects of extreme climate on vegetation in China in terms of scale and spatial heterogeneity? (2) What are the leading factors in different regions? The aim of this study is to be helpful in the further understanding of the relationship between climate and the terrestrial carbon cycle, and to contribute a crucial study case to future research in the field of global extreme climate on “attribution”, “detection” and “impact” by exploring the relationship between extreme climate conditions and vegetation in China. Moreover, we hope to provide a basis for adopting scientific countermeasures according to local conditions through identifying the regional differences in the impacts of various extreme climate indices on vegetation.

2. Materials and Methods

2.1. Data Sources

2.1.1. Meteorological Data

We used the daily observational temperature and precipitation data from 2474 national surface meteorological stations in China, provided by the National Information Center of China Meteorological Administration. After data screening and processing, the influences of meteorological station migration and missing data were eliminated, and 1698 meteorological stations nationwide were ultimately retained as research objects (Figure 1).

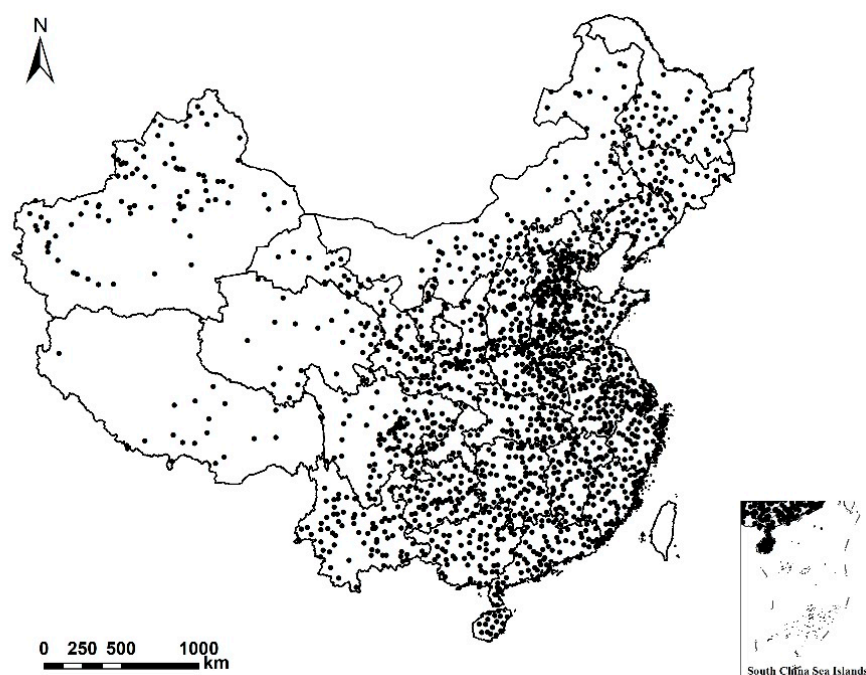


Figure 1. Distribution map of meteorological stations in China used in the study.

2.1.2. Normalized Difference Vegetation Index

The Normalized Difference Vegetation Index (NDVI) is a vegetation index based on the difference in the spectral reflectance characteristics of the leaves in red (visible) and near-infrared bands. It can monitor the vegetation growth and coverage changes well and provide information on the structure and greenness of the plant. The NDVI data we used came from the Moderate Resolution Imaging Spectroradiometer (MODIS) on NASA's Terra and Aqua satellites. In this study, MODIS NDVI's latest sixth generation product MOD13C2 was used. This set contains monthly data with a spatial resolution of $0.05^\circ \times 0.05^\circ$. The data were downloaded from the official website of the NASA Land Processes Distributed Active Archive Center (<https://lpdaac.usgs.gov/>, accessed on 2 June 2020). The original data were processed with atmospheric correction (including cloud and aerosol disturbance removal, etc.) and subjected to strict quality control [25]. The spatial distribution patterns of MODIS NDVI were consistent with the distribution characteristics of vegetation in China, thus we can use the data directly without any transformation.

2.1.3. Climate Zone

China has a vast territory and spans multiple temperature zones. The dry and wet conditions in different regions also differ. Therefore, in the analysis of the results, the climate zoning information, with comprehensive consideration of temperature and moisture, was used to determine the hydrothermal background of the climate to supplement the description of the location (Figure 2) [26].

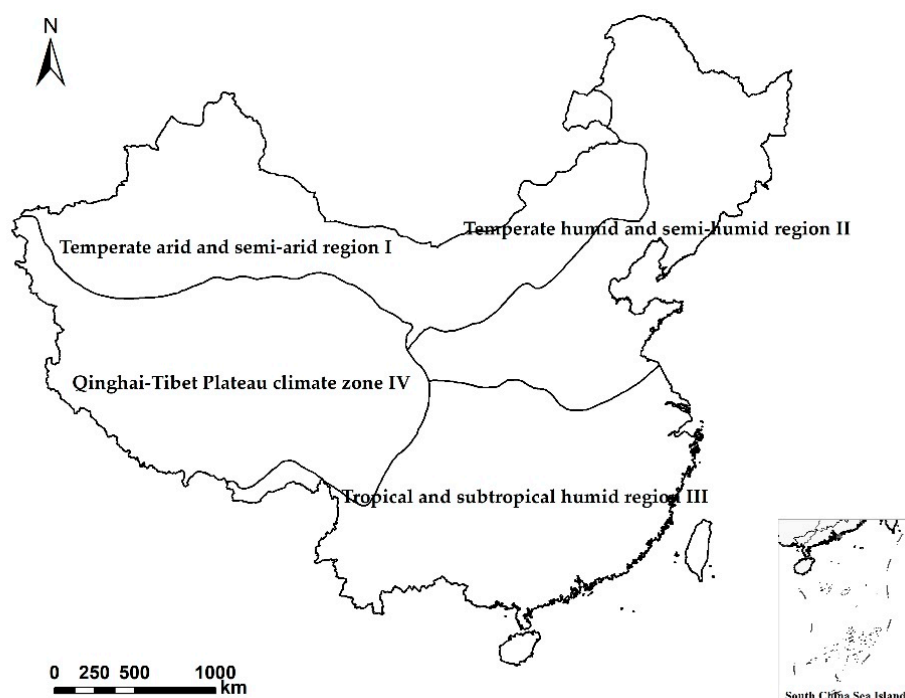


Figure 2. Climate zone map of China.

Considering the availability of both the MODIS NDVI and meteorological data sources, we finally chose 2001–2018 as the research period. According to the growth characteristics of most vegetation types in China, and the research experience on vegetation in China, we used April to October as the growing season to study the effects of extreme climate on vegetation.

2.2. Methodology

2.2.1. Selection of Representative Extreme Climate Indices

Using Climpack2, we calculated the 27 extreme climate indices of the ETCCDI via the meteorological data in batches. Climpack2 was developed by the WMO Climate Council Expert Group [27]. After this calculation, we conducted a correlation analysis between the extreme climate indices and NDVI. According to this analysis, NDVI was not significantly correlated with the number of warm days (WSDI) and cold days (CSDI) in the growing seasons from 2001 to 2018. The definitions of the 27 indices and regression analysis results are listed in Table S1 in Supplementary Materials.

In order to further exclude the influence of collinearity among extreme climate indices in the regression model, a multi-collinearity diagnosis was performed in Statistical Product and Service Solutions (SPSS) for the other extreme climate indices, after removing the indices showing no significant correlation. Those variables with a variance inflation factor (VIF) below 10 in the collinearity statistics were retained. According to these results, we finally chose two extreme temperature indices and three extreme precipitation indices. These were TX_x , TX_{10p} , CDD, CWD and $R95pTOT$. The five indices are defined in Table 1.

Table 1. Definition of the five selected extreme climate indices of ETCCDI.

Indices	Definition	Unit
TX _x	Monthly maximum value of daily maximum temperature	°C
TX10p	Percentage of days when daily maximum temperature < 10th percentile	%
CDD	Maximum length of dry spell, maximum number of consecutive days with daily precipitation amount < 1 mm	d
CWD	Maximum length of wet spell, maximum number of consecutive days with daily precipitation amount ≥ 1 mm	d
R95pTOT	Annual total precipitation when daily precipitation amount > 95th percentile	mm

Information come from http://etccdi.pacificclimate.org/list_27_indices.shtml (accessed on 1 December 2020).

2.2.2. Multiscale Geographically Weighted Regression

The traditional global regression model (GRM) assumed that the relationship between spatial variables was fixed such that it did not change with location, which was obviously not consistent with the actual situation. The geographically weighted regression (GWR) model and multiscale geographically weighted regression (MGWR) model were proposed to resolve this contradiction. According to the Tobler's first law of geography, "everything is related to everything else, but near things are more related than distant things" [28], and in the GWR and MGWR model, "borrowed" data from points at nearby locations were used to make the regression varied across space. The data-borrowing range was identified as "bandwidth". Detail information can be learned from the related literature [29–34]. Compared with GWR, which employs the same optimal bandwidths for different independent variables [29–32], the MGWR method allows for changes in the relationship between the independent variable and dependent variable with shifts in spatial location, and can also calculate the optimal bandwidths of each independent variable in relation to the dependent variable; that is, the effective scale of the spatial relationship. Accordingly, the simulation results of this model are closer to the actual situation [33]. This method can not only analyze the spatial correlation of data, but can also identify the spatial heterogeneity of relationships. The two processes of spatial analysis can be combined to quantitatively evaluate the magnitude of the spatial differences.

In this study, the vegetation index was taken as the dependent variable and the extreme climate index as the independent variable. The MGWR method was used to evaluate the spatial scale of the impacts of extreme temperature and precipitation on vegetation, and to explore the spatial heterogeneity of these impacts. The selected indicators of the model are the quadratic kernel function and the AICc information criterion. We chose SOC-f as the iterative termination criterion because it not only focuses on the overall model fit, but compared with SOC-RSS, it can also better detect the relative changes in each additive terms [33].

We used the spatial analyst tools "Extract Multi Values to Points" based on bilinear interpolation in ArcGIS to extract the NDVI of each station from the raster data source of MODIS NDVI. Then, we calculated the regression coefficients between NDVI and extreme climate indices in MGWR2.2 software [34]. The extreme climate indices and NDVI analyzed were both based on annual mean data of the growing season from 2001 to 2018.

2.2.3. Self-Organizing Feature Map

The self-organizing feature map (SOFM) was first proposed by Kohonen, a Finnish scholar, based on the theory of cortical competition (lateral inhibition). It is a kind of unsupervised learning neural network. This kind of neural network does not need to be informed the output associated with the input mode in advance. It is also not necessary to give it the category's expected value in advance; instead, it learns and evolves through different parts of the network in response to different input modes, and can extract the

corresponding features and rules, which are reflected in space as samples with the same or similar features being concentrated in a certain region [35].

The topology structure of the SOFM network is a fully interconnected neuron array composed of two layers: the input layer and the competitive layer (Figure 3). The input layer is used to receive input samples, and the input samples are classified in the competitive layer. The specific learning process of the SOFM primarily involves the initialization and training of the network. The training process of the network involves adjusting the weights of the neurons in the competitive layer. The arrangement of neurons in the competitive layer is specified by the topological function, and the distance between neurons is calculated by the distance function.

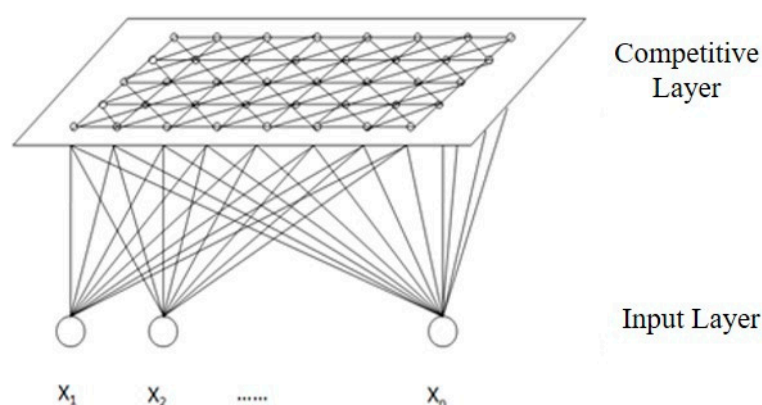


Figure 3. The topology of the SOFM network.

The SOFM network does not need to make judgment and weight setting in advance, and is not affected by subjective judgment. Therefore, it has been widely used in cluster analysis. Based on the results of single factor analysis of the impact of extreme climate on vegetation in the MGWR model, this paper uses the SOFM network to conduct cluster analysis to identify the dominant influence factor and the component effects of multiple extreme climate indices on vegetation in China. In this study, we used the normalized regression coefficients of different extreme climate indices from each station as samples and input them into the SOFM network for training.

3. Results

3.1. Impacts of Extreme Climate Indices on NDVI and Its Spatial Heterogeneity in China

3.1.1. Performance of MGWR Model

Taking the annual average NDVI of the growing season from 2001 to 2018 as the dependent variable and the five extreme climate indices as the independent variables, the regression was conducted in the MGWR2.2 software. The model's statistical results are shown in Tables 2 and 3. Adj- R^2 , RSS and AICc are the three most important indicators for measuring the fitting effect of the regression model. The larger Adj- R^2 is, the higher the goodness-of-fit of the model will be, while the smaller the RSS and AICc are, the better the performance of the regression model will be. It can be seen from Table 2 that among the three models, MGWR has the best performance.

Table 2. Performance comparison of different models.

Indicator	GRM	GWR	MGWR
Adj- R^2	0.654	0.852	0.857
RSS	585.304	225.466	201.764
AICc	3025.058	1902.813	1776.306

Table 3. Bandwidth comparison of MGWR and GWR models.

Variables	Bandwidth	
	MGWR	GWR
TX _x	871	77
TX10p	99	77
CDD	69	77
CWD	426	77
R95pTOT	1321	77
Intercept	43	77

Nationwide, the bandwidth of the GWR model was 77, which means that the spatial scale of the effect of different extreme indices was the same. Other than this, the impacts of different kinds of extreme climate indices all operated on the local scale. However, the MGWR model is flexible in terms of the optimal scale, and each independent variable corresponds to a different bandwidth. Different extreme climate indices have different spatial scale effects on the vegetation NDVI (Table 3). In the MGWR model, the statistical results of the bandwidth of each variable were as follows: R95pTOT > TX_x > CWD > TX10p > CDD. CDD showed the greatest spatial heterogeneity, while R95pTOT had the greatest spatial stability.

3.1.2. Spatial Heterogeneity Analysis of the Impacts of Extreme Climate Indices on NDVI

Variable standardization was performed before the model was operated. This renders the regression coefficients of each variable dimensionless, meaning they can be compared in detail, as in Table 4. More sites passed the significance test in the context of the effect of extreme precipitation than in the context of extreme temperature, which indicates that extreme precipitation had a broader influence on vegetation in China in the 18 years studied. The regression coefficients of CWD passed the significance test for all sites, meaning that CWD had a significant impact on the vegetation of the whole country. The regression coefficients of CWD and R95pTOT are both positive, indicating that the increase in extreme precipitation over the 18 years studied—both the number of precipitation days and the amount of precipitation—caused an increase in NDVI all over the country. After the significance screening of TX_x, all of the regression coefficients were also positive. The regression coefficients of CDD and TX10p have both positive and negative values, which need to be correlated to their spatial distribution in the site for analysis. CDD and CWD show large mean regression coefficients and high degrees of influence.

Table 4. Regression coefficient data for different variables in the MGWR model.

Variable	Mean	Mean Value after Significance Test	Min	Minimum Value after Significance Test	Max	Maximum Value after Significance Test	Proportion of Sites that Pass the Significance Test
TX _x	0.073	0.124	−0.033	0.059	0.207	0.207	47.56%
TX10p	0.113	0.181	−0.417	−0.417	0.401	0.401	48.38%
CDD	−1.1	−1.626	−3.308	−3.308	1.237	1.237	68.51%
CWD	0.656	0.656	0.261	0.261	1.024	1.024	100%
R95pTOT	0.054	0.066	0.023	0.038	0.092	0.092	67.92%

The spatial pattern of the regression coefficients of each extreme climate variable is shown in Figure 4. As regards the impacts of TX_x on vegetation, the sites in Northeast China, North China, the middle and lower reaches of the Yangtze River, and the southeast coastal areas did not pass the significance test. In the sites that passed the significance test, the TX_x was positively correlated with vegetation growth, and the degree of influence gradually increased from east to west. The spatial scale of the effects was large (regional).

The direction of influence was the same at all the stations that passed the significance test, but the degrees of impact varied between regions.

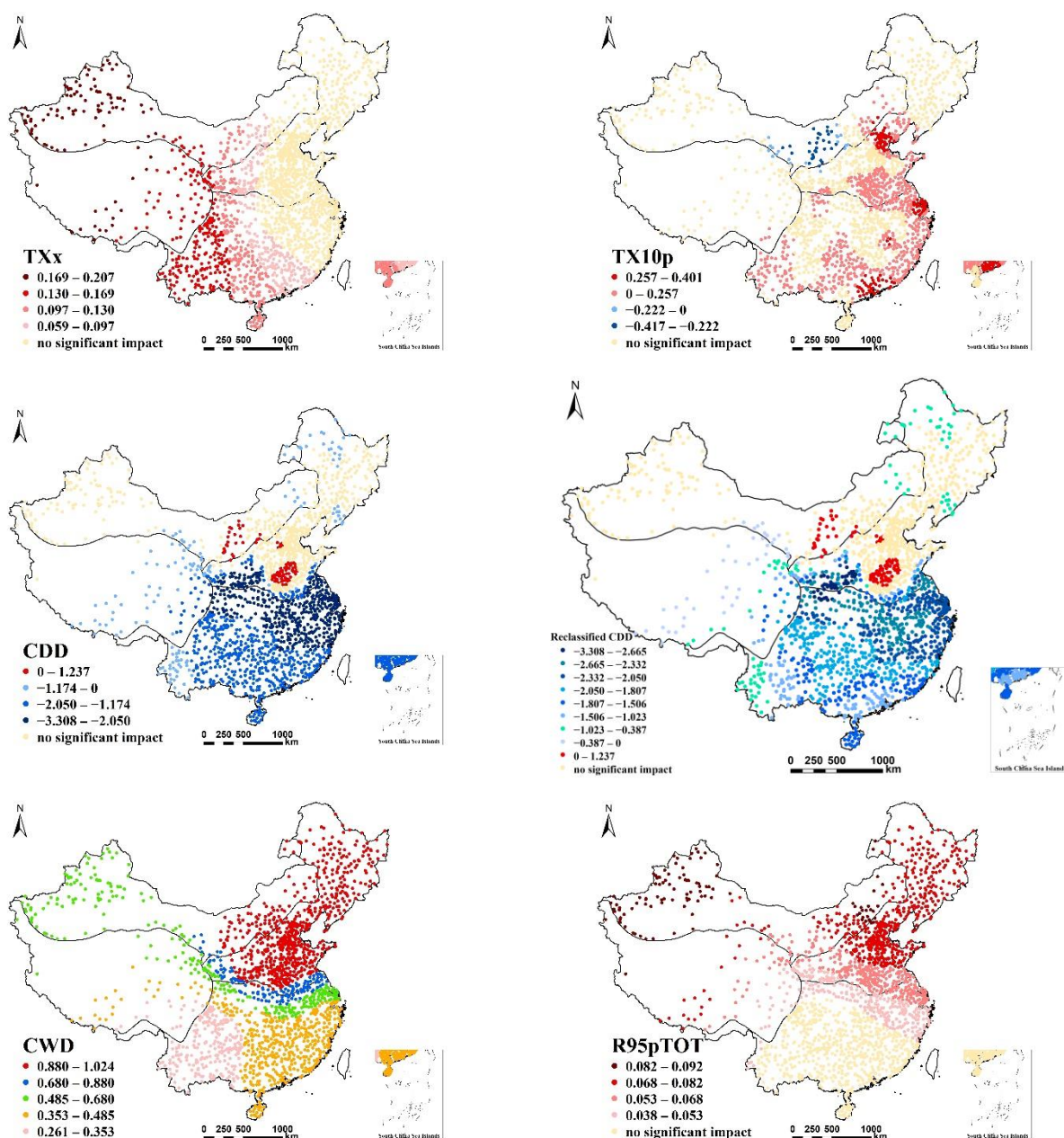


Figure 4. Spatial pattern of the impact of five extreme climate indices on NDVI in China.

The spatial difference of TX10p was greater than in TX_x. Among the stations that passed the significance test, the regression coefficients of the sites in the upper and middle reaches of the Yellow River were all negative, especially in the Hetao plain area. In the analysis of TX_x, the correlation coefficient was positive in this area. The NDVI is elevated under higher temperatures, and inhibited by lower temperatures. Evidently, the area is more vulnerable to cold waves, frost, and other extreme cold events. The other regions that passed the significance test were all positively correlated, and the spatial scale pattern was mainly local. The areas with relatively large regression coefficients are concentrated in the Beijing–Tianjin–Hebei region, the Yangtze River Delta and the Pearl River Delta, all of which are economically developed districts with high population densities. TX10p has

a small bandwidth, only slightly larger than that of CDD, which means that the impact of TX10p on NDVI has very strong spatial heterogeneity. In practice, the impact of TX10p should be considered locally.

CDD has the smallest bandwidth among the five indicators, and thus the most apparent spatial heterogeneity. In terms of spatial distribution, the sites that failed to pass the significance test are mainly located in the north, including Northeast China, North China and Xinjiang province of China. The vegetation in these areas was not significantly affected by consecutive drought days in the 18 years studied. The number of sites positively correlated with NDVI is relatively small, and these sites are concentrated in the Hetao Plain in the middle and upper reaches of the Yellow River, and the Huanghuai Plain in its lower reaches. The vegetation in these areas showed a strong adaptability to drought. The sites with negative regression coefficients are mainly distributed in the southern region, and the degree of influence decreases gradually from north to south and from east to west. The north and south of Northeast China and some areas of Inner Mongolia also contain areas that were impacted negatively. The plotting grade differences in CDD reached about 1.1, even though this feature showed a basically regional character. If the grade differences were narrow, a patchier spatial distribution would be obtained (see reclassified CDD), with very high spatial heterogeneity.

The spatial effects of CWD on vegetation are relatively regular. From southwest to northeast, the degree of influence on vegetation gradually deepens. There is some spatial heterogeneity, but its scale is relatively large. The promotional influence of CWD on vegetation during the growing season in the studied period is regional.

The bandwidth of R95pTOT is the largest, while its spatial heterogeneity is the smallest. Southern China generally failed the significance test; the regression coefficients of central and northern China showed an increasing trend from south to north, and the regression coefficient of the Xinjiang region was the highest in China. The difference between the maximum value and the minimum value of the R95pTOT regression coefficient is only 0.054, meaning that if the mapping grade is more than 0.054, there will be no spatial heterogeneity. Accordingly, the spatial heterogeneity of this index in China is very small. The influence of R95pTOT is national.

3.2. The Dominant Factors and Regional Characteristics of the Impact of Extreme Climate on NDVI

In this section, R95pTOT, which showed no apparent spatial difference in China, was removed, and the regression coefficients of the other four extreme climate indices and vegetation indices were used as clustering indices. The regression coefficients were inputted into the SOFM network for training, until the topology of the network remained basically unchanged. Given that this analysis seeks to identify the dominant elements in each category and the significance of influence, the number of categories was set as five.

3.2.1. Clustering Results and Test

The spatial pattern of the clustering results affecting NDVI is shown in Figure 5. The spatial agglomeration characteristics of the five types are obvious. Type 1 is mainly distributed in the Northeast Plain and the North China Plain, in the temperate humid and semi-humid regions, and in the eastern parts of the temperate arid and semi-arid regions. Type 2 is distributed in the southern part of the tropical and subtropical humid areas of Guangdong Province, and on the boundaries of Guangdong and Fujian, Hunan and Guangxi, and Hunan and Guizhou. Type 3 is mainly concentrated in the north and east of the tropical and subtropical humid regions, such as the middle and lower reaches of the Yangtze River plain and the surrounding area. Type 4 is located in the Qinghai-Tibet Plateau and the transitional zone between the region and tropical and subtropical humid areas, including the southeastern part of the Qinghai-Tibet Plateau, the Sichuan Basin, the Yunnan-Guizhou Plateau, most of Guangxi, the Leizhou Peninsula, and Hainan Island. Type 5 is mainly located in the central and western areas of the temperate arid

and semi-arid regions, the northeastern part of the Qinghai–Tibet Plateau, and most of the Loess Plateau.

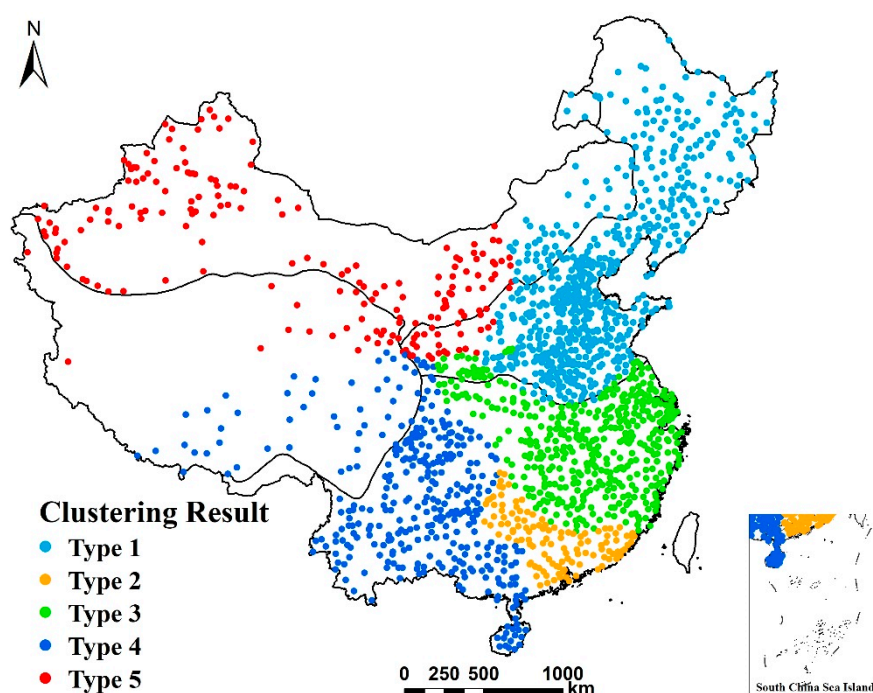


Figure 5. Clustering results of the impact of extreme climate on NDVI based on the SOFM network.

In order to test the rationality of our classification, one-way ANOVA was performed in SPSS to test whether there were significant differences among all five types, as well as between sets of two types. Given space restraints, we have only listed the results for CDD as a table, and the rest of the indices will be described.

Following the overall analysis of variance (Table 5), the significance test results of the impact of the four extreme climate indices on NDVI were all less than 0.01, suggesting extreme significance. There were extremely significant differences among the five types, indicating that the classification was generally scientific and reasonable. According to the results of the multiple variance analysis of the impact of CDD on NDVI (Table 6), there were no significant differences in the effects of CDD between Type 1 and Type 5, or between Type 2 and Type 4, since they did not pass the significance test. However, all the other pairs showed significant variation in terms of the influence of CDD. The five types of impacts of CWD, TX10p and TX_x all passed the pairwise significance test, with significant differences.

Table 5. Overall variance analysis of the effect of CDD on NDVI.

	Sum of Squares	df	Mean Square	F	Sig.
Between Groups	1451.407	4	362.8517	930.2601	0.000
Within Groups	660.7516	1694	0.390054		
Total	2112.158	1698			

Table 6. Multiple variance analysis of the effect of CDD on NDVI.

(I) 5 Types	(J) 5 Types	Mean Difference (I-J)	Std. Error	Sig.	95% Confidence Interval	
					Lower Limits	Upper Limits
1	2	1.53925 *	0.06260	0.00000	1.41646	1.66204
	3	2.13345 *	0.03925	0.00000	2.05648	2.21043
	4	1.42263 *	0.04194	0.00000	1.34036	1.50489
	5	−0.01401	0.05201	0.78768	−0.11603	0.08801
2	1	−1.53925 *	0.06260	0.00000	−1.66203	−1.41646
	3	0.59421 *	0.06463	0.00000	0.46745	0.72096
	4	−0.11662	0.06630	0.07876	−0.24665	0.01342
	5	−1.55326 *	0.07309	0.00000	−1.69660	−1.40991
3	1	−2.13345 *	0.03925	0.00000	−2.21043	−2.05648
	2	−0.59421 *	0.06463	0.00000	−0.72096	−0.46745
	4	−0.71082 *	0.04490	0.00000	−0.79890	−0.62275
	5	−2.14746 *	0.05443	0.00000	−2.25422	−2.04071
4	1	−1.42263 *	0.04194	0.00000	−1.50490	−1.34036
	2	0.11662	0.06630	0.07876	−0.013417	0.24665
	3	0.71082 *	0.04490	0.00000	0.62275	0.79890
	5	−1.43664 *	0.05640	0.00000	−1.54727	−1.32601
5	1	0.01401	0.05201	0.78768	−0.08801	0.11603
	2	1.55326 *	0.07309	0.00000	1.40991	1.69660
	3	2.14746 *	0.05443	0.00000	2.04071	2.25422
	4	1.43664 *	0.05640	0.00000	1.32601	1.54727

* The significance level of mean difference was 0.05.

3.2.2. Analysis of the Regional Dominant Factors of the Impact of Extreme Climate on NDVI

On the basis of the above classification test, the difference between the mean value of the regression coefficients of different extreme climate indices in each type and the national mean value was calculated to judge the magnitude of the impact. The results are shown in Figure 6. For the convenience of comparison, the difference in CDD was calculated after taking the absolute value of the regression coefficient into account. Through the size of the value of difference, we can judge the “intensity” of the impact of the extreme climate index on vegetation. Based on the results of the analysis of regression coefficients, the regression coefficients of some sites did not pass the significance test (their influence was not significant). Therefore, the significance test should be taken into consideration when identifying specific features of each type. We calculated the percentage of sites that passed the significance test for the different extreme climate indices in each type. The results are shown in Figure 7. According to the proportion, the impact scope of each extreme climate index on vegetation in different types can be identified. At the same time, the proportion can be used to examine the results of impact intensity. The elements with a higher proportion of sites passing the significance test and greater influence intensity are the dominant ones.

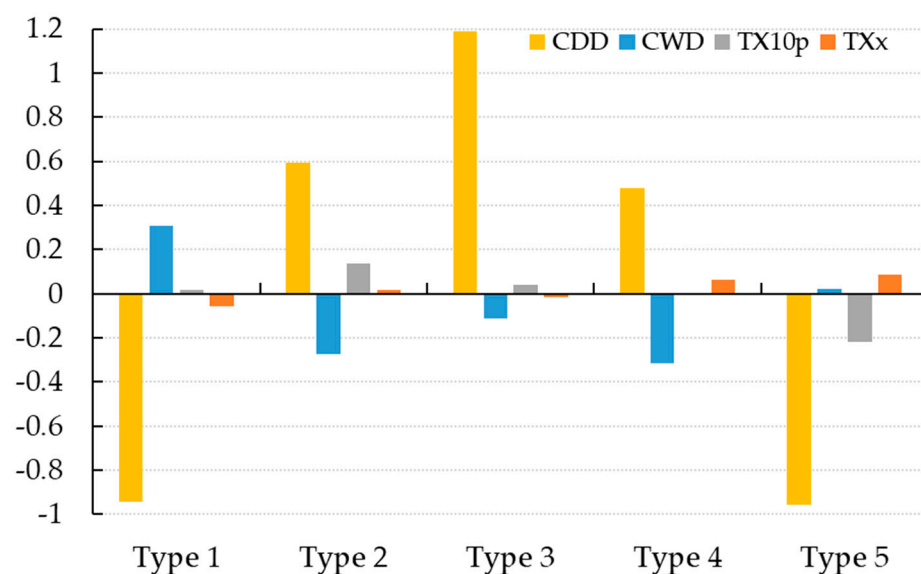


Figure 6. Statistical graph of regression coefficient for the anomaly results.

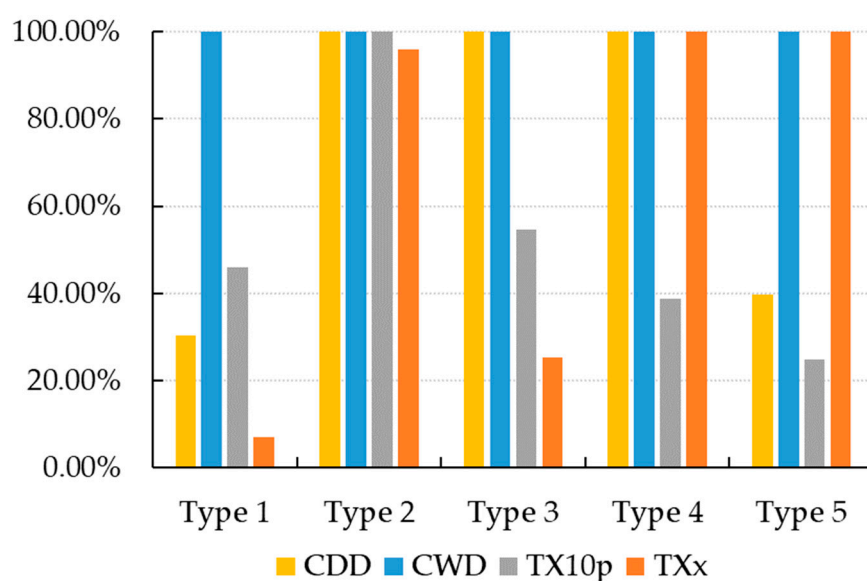


Figure 7. Statistical chart of the proportion of sites that passed the significance test.

In Type 1, as regards the influence of CWD, the proportion of sites passing the significance test is the highest, reaching 100%. The proportions of each of the other three extreme climate indices are below 50%. In this region, CWD has the largest influence scope on vegetation. In the assessment of difference, the influence intensities of CWD and TX10p are both higher than the national average, but the degree of deviation of TX10p is low. In general, the NDVI in this area was mainly affected by CWD, in terms of both geographical area and intensity, in the 18 years studied.

In Type 2, all sites passed the significance test for CDD, CWD and TX10p, but not TXx, for which this proportion was slightly lower. Besides CWD, the degree of influence of the other three indices were all higher than the national average, among which CDD had the largest influence. As shown by the horizontal comparison of the five types, TX10p in Type 2 is present at the highest level, and has the greatest influence among the five types. In general, the Type 2 region is mainly affected by CDD and TX10p.

In Type 3, the proportion of CDD and CWD sites passing the significance test was 100%, followed by TX10p. In terms of influence intensity, CDD and TX10p were above the

national average, and the deviation of CDD was the most obvious and was the greatest among the five types. In short, the vegetation in this region was mainly affected by CDD in the 18 years studied.

In Type 4, all extreme climate indices except for TX10p at all sites passed the significance test (100%), and a large range of influence was shown in this region. The influence intensity of both CDD and TX_x was higher than the national average. CDD showed the strongest intensity in this region, and the influence intensity of TX_x here was second only to this feature's intensity in Type 5, which is the region most affected by TX_x. In conclusion, the vegetation in the Type 4 region was strongly affected by CDD and TX_x.

Type 5 is mainly influenced by CWD and TX_x in spatial scope, and the sites of both indices passed the significance test up to 100%. In this region, the CDD was below the national average, and showed a higher degree of deviation, close to that of Type 1, which also explains why there was no significant difference in CDD between Type 1 and Type 5 according to the multiple analyses of variance. The value of CWD was higher than the national average, and its influence intensity was second only to that of Type 1, which showed a strong influence. TX_x showed the greatest change in intensity. Considering the proportion of sites passing the significance test, and the intensity of influence, we can assert that the vegetation in this area is mainly affected by the compound influence of CWD and TX_x.

Based on the results of the comprehensive type analysis, those factors with a degree of influence above the national average are labeled "+", and those whose influence degree deviates significantly are labeled "++". Those below the national average are marked "-", and those deviating significantly are marked "--" (Table 7). According to the characteristics of the different dominant factors, the five types can be described as follows: the humidity-promoting type; the cold-promoting and drought-inhibiting compound type; the drought-inhibiting type; the heat-promoting and drought-inhibiting compound type, and the heat-promoting and humidity-promoting compound type. Correspondingly, vegetation in different areas can be susceptible to the adverse effects of different extreme climate events in the future. In the Type 1 areas, the vegetation was mainly enhanced by extreme precipitation, which means that the vegetation in this area is more adapted to the humid environment. As such, this type will be more sensitive to drought in the future. Type 2, showing an increase in TX10p, showed higher NDVI and a better vegetation condition. However, this is inhibited by CDD. Therefore, in this region, we should pay more attention to preventing the risks of heat wave and drought. Type 3 was shown to not be significantly affected by other indices, and was mainly inhibited by drought (the factor with the highest intensity). In the future, dry conditions caused by the intensification of extreme drought in this region should be addressed. Type 4 showed similar properties to Type 2: it is an area affected simultaneously by extreme temperature and extreme precipitation. This area was shown to be subjected to obvious inhibitory effects by drought, which verifies the multiple analysis of variance for these two types in terms of CDD. Compared to Type 2, the vegetation in Type 4 regions was mainly enhanced by heat events, implying the higher risk of extreme cold events in the future. Type 5 is also a composite type, which is enhanced by high temperatures and is at high risk of damage as a result of cold waves in the future. Meanwhile, the extreme precipitation level also promotes the growth of vegetation in this region. If the extreme precipitation decreases, the vegetation is more likely to be inhibited, and so the risk of drought to vegetation here is high. In general, Type 2, Type 4 and Type 5 are all under the compound influence of extreme temperature and extreme precipitation, while Type 1 and Type 3 are influenced primarily by single factors.

Table 7. Comprehensive description of the impact types and future risks of extreme climate in terms of NDVI, identified via the SOFM network.

Type	Description of the Type	Main Risk in the Future	CDD	CWD	TX10p	TX _x
1	Humidity-Promoting Type	Drought	— —	++	+	— —
2	Cold-Promoting and Drought-Inhibiting Compound Type	Hot wave, Drought	++	— —	++	+
3	Drought-Inhibiting Type	Drought	++	—	+	—
4	Heat-Promoting and Drought-Inhibiting Compound Type	Cold wave, Drought	++	— —	—	++
5	Heat-Promoting and Humidity-Promoting Compound Type	Cold wave, Drought	— —	++	— —	++

4. Conclusions and Discussion

In this study, representative extreme climate indices were selected to explore the spatial heterogeneity and complexity of the impacts of extreme climate on the greenness of vegetation in China, during the growing seasons in the years from 2001 to 2018. The main conclusions are as follows:

- (1) There were spatial differences in the impacts of climate extremes on vegetation, and there were obvious scale effects of different extreme climate indices. Among the five extreme climate indices, the effects of CDD and TX10p on vegetation were small in the spatial scale, and their spatial heterogeneity was strong. Therefore, regional studies should be focused on high-risk areas. R95pTOT showed a large spatial scale, and its scale of influence was close to the whole country. Therefore, more attention should be paid to the overall, national-scale changes. Under current extreme climatic conditions, the scope of the impact of extreme precipitation on vegetation in China is larger, and the increase in extreme precipitation in most regions is beneficial to vegetation growth, while the effect of extreme temperature is relatively complex;
- (2) During the period 2001–2018, the impacts of extreme climate on NDVI in China showed obvious regional characteristics. The spatial classification results describe two single-factor types (humidity-promoting and drought-inhibiting), and three combination types (cold-promoting and drought-inhibiting, heat-promoting and drought-inhibiting, heat-promoting and humidity-promoting), of the impact of extreme temperature and precipitation. The results show that drought is a typical extreme climate risk for vegetation growth in China;
- (3) The study identified some sensitive areas, such as the Beijing–Tianjin–Hebei region, the Yangtze River Delta, and the Pearl River Delta, which are more adaptable to extreme low temperature. Vegetation in these areas is more likely to be affected by high temperature and heat waves in the future. The vegetation in Hetao Plain was inhibited by extreme low temperature and promoted by drought conditions, which was different from other regions in China, and should be paid more attention.

The conclusions of this study are verified by the results of other studies on typically affected regions and representative extreme temperature and precipitation events in China. Our results are consistent with Zhang et al. [36], who conducted a comparative study in the dryland ecosystem between Xinjiang and Arizona on the response of natural vegetation to climate. Based on their research, they concluded that vegetation growth in Xinjiang was positively correlated with wet conditions based on the increase in precipitation. This is consistent with our conclusion that the CWD and R95pTOT, which represent the humidity conditions, all had a positive relationship with the NDVI. Zhang et al. indicated that large fraction of Xinjiang experienced warming and wetting, which is exactly the same as our conclusion for Xinjiang area in the SOFM simulation work, that the impact type of extreme climate to the vegetation in Xinjiang was heat-promoting and humidity-promoting compound. In addition, we all gave the judgement that the drought will be a major risk

in the future in this area. Similar conclusions to our study were also made in the research carried out by Abbas et al. [37] on the Pearl River Delta in China, in that for the growing season from 1982 to 2015, temperature was negatively correlated with crop production and forest vegetation, which corresponds with our conclusion, especially with the results of SOFM. The study of Chu et al. [38] drew the conclusion that precipitation was the dominant effect factor on NDVI during the growing season in the Amur-Heilongjiang River Basin based on GIMMS NDVI and raster climate data source, which verified our results in Northeast China.

This study also performed a comprehensive and systematic analysis of the spatial differences in the impacts of extreme climate on vegetation at the national scale, providing a basis for the prevention of extreme climate risks according to local conditions. Compared with previous studies using global regression or GWR models, the spatial scale of impacts in this study is more quantitative and precise. The spatial scale of the impacts corresponding to each extreme climate index is analyzed, and the conclusions of the spatial analysis are optimized. At the same time, in our comprehensive analysis of the regionally dominant factors, the boundaries and the weights of indicators are not defined in advance. Instead, the principle of the artificial neural network is used to conduct a classification analysis from the perspective of the data's structure similarity, so as to avoid the interference of subjective experience. The results call attention to drought, which threatened the entire country. Meanwhile, heat waves and cold waves pose risks for some regions in the future that should be paid more attention in practice.

In this study, only the NDVI was considered. Some studies assert that the NDVI mainly represents structural information, such as vegetation coverage and greenness, but cannot accurately reflect the physiological activity of vegetation. The conclusions related to physiological functions, such as the length of the growing season, analyzed by NDVI are different from the actual observational results [39–41]. With the progress made in remote sensing technology and the detection of fluorescence, solar-induced chlorophyll fluorescence (SIF), as a by-product of photosynthesis, has gradually attracted attention in the field of vegetation research due to its ability to represent physiological activities related to photosynthesis [42–46]. In the future, we may be able to introduce SIF into the practice of vegetation representation, in order to study the impacts of extreme climate on vegetation in a more comprehensive way. In addition, the aim of this study was to systematically evaluate the spatial influence characteristics of extreme climate on vegetation, and so a discussion of human influence is not included. In future study, the contributions of climate and human activities to vegetation change can be comprehensively discussed for different regions, based on the typical regions identified in this study.

Supplementary Materials: The following are available online at <https://www.mdpi.com/article/10.3390/su13105748/s1>, Figure S1: Map of provinces in China, Table S1: Definitions of the 27 extreme climate indices of ETCCDI and the results of correlation analysis.

Author Contributions: Conceptualization, S.L. (Shuang Li), F.W. and S.L. (Shuangcheng Li); Data curation, S.L. (Shuang Li), F.W., Z.W., J.S. and Z.L.; Formal analysis, S.L. (Shuang Li); Funding acquisition, S.L. (Shuangcheng Li); Investigation, S.L. (Shuang Li) and F.W.; Methodology, S.L. (Shuang Li) and F.W.; Project administration, S.L. (Shuangcheng Li); Software, S.L. (Shuang Li), F.W., Z.W. and J.S.; Supervision, S.L. (Shuangcheng Li); Validation, S.L. (Shuang Li), F.W., Z.L., H.W. and S.L. (Shuangcheng Li); Visualization, S.L. (Shuang Li), F.W. and J.S.; Writing—Original draft, S.L. (Shuang Li); Writing—Review and editing, S.L. (Shuang Li), F.W. and S.L. (Shuangcheng Li). All authors have read and agreed to the published version of the manuscript.

Funding: This research was funded by the Major Projects of the National Natural Science Foundation of China, grant number 41590843.

Institutional Review Board Statement: Not applicable.

Informed Consent Statement: Not applicable.

Data Availability Statement: Not applicable.

Acknowledgments: We thank the Major Projects of the National Natural Science Foundation of China (No. 41590843) for its support. We thank all the data source provider of this paper. We are also grateful to the editor and the reviewers for their helpful comments.

Conflicts of Interest: The authors declare no conflict of interest.

References

1. IPCC. *Managing the Risks of Extreme Events and Disasters to Advance Climate Change Adaptation: A Special Report of Working Groups I and II of the Intergovernmental Panel on Climate Change*; Cambridge University Press: Cambridge, NY, USA, 2012.
2. Shafran-Nathan, R.; Svoray, T.; Perevolotsky, A. Continuous droughts' effect on herbaceous vegetation cover and productivity in rangelands: Results from close-range photography and spatial analysis. *Int. J. Remote Sens.* **2013**, *34*, 6263–6281. [\[CrossRef\]](#)
3. Forzieri, G.; Cescatti, A.; Silva, F.B.; Feyen, L. Increasing risk over time of weather-related hazards to the European population: A data-driven prognostic study. *Lancet Planet. Health* **2017**, *1*, e200–e208. [\[CrossRef\]](#)
4. Liu, D.; Wang, T.; Yang, T.; Yan, Z.; Liu, Y.; Zhao, Y.; Piao, S. Deciphering impacts of climate extremes on Tibetan grasslands in the last fifteen years. *Sci. Bull.* **2019**, *64*, 446–454. [\[CrossRef\]](#)
5. Schuldt, B.; Buras, A.; Arend, M.; Vitasse, Y.; Beierkuhnlein, C.; Damm, A.; Gharun, M.; Grams, T.E.; Hauck, M.; Hajek, P.; et al. A first assessment of the impact of the extreme 2018 summer drought on Central European forests. *Basic Appl. Ecol.* **2020**, *45*, 86–103. [\[CrossRef\]](#)
6. Le Quéré, C.; Raupach, M.R.; Canadell, J.G.; Marland, G.; Bopp, L.; Ciais, P.; Conway, T.J.; Doney, S.C.; Feely, R.A.; Foster, P.; et al. Trends in the sources and sinks of carbon dioxide. *Nat. Geosci.* **2009**, *2*, 831–836. [\[CrossRef\]](#)
7. Sanz-Lázaro, C. Climate extremes can drive biological assemblages to early successional stages compared to several mild disturbances. *Sci. Rep.* **2016**, *6*, 30607. [\[CrossRef\]](#)
8. Wernberg, T.; Bennett, S.; Babcock, R.C.; De Bettignies, T.; Cure, K.; Depczynski, M.; Dufois, F.; Fromont, J.; Fulton, C.J.; Hovey, R.K.; et al. Climate-driven regime shift of a temperate marine ecosystem. *Science* **2016**, *353*, 169–172. [\[CrossRef\]](#)
9. Harris, R.M.B.; Beaumont, L.J.; Vance, T.R.; Tozer, C.R.; Remenyi, T.A.; Perkins-Kirkpatrick, S.E.; Mitchell, P.; Nicotra, A.B.; McGregor, S.; Andrew, N.R.; et al. Biological responses to the press and pulse of climate trends and extreme events. *Nat. Clim. Chang.* **2018**, *8*, 579–587. [\[CrossRef\]](#)
10. Verrall, B.; Pickering, C.M. Alpine vegetation in the context of climate change: A global review of past research and future directions. *Sci. Total. Environ.* **2020**, *748*, 141344. [\[CrossRef\]](#)
11. Teuling, A.J.; Seneviratne, S.I.; Stöckli, R.; Reichstein, M.; Moors, E.; Ciais, P.; Luyssaert, S.; Hurk, B.V.D.; Ammann, C.; Bernhofer, C.; et al. Contrasting response of European forest and grassland energy exchange to heatwaves. *Nat. Geosci.* **2010**, *3*, 722–727. [\[CrossRef\]](#)
12. Rammig, A.; Wiedermann, M.; Donges, J.F.; Babst, F.; Von Bloh, W.; Frank, D.; Thonicke, K.; Mahecha, M.D. Coincidences of climate extremes and anomalous vegetation responses: Comparing tree ring patterns to simulated productivity. *Biogeosciences* **2015**, *12*, 373–385. [\[CrossRef\]](#)
13. Xie, Z.; Huete, A.; Cleverly, J.; Phinn, S.; McDonald-Madden, E.; Cao, Y.; Qin, F. Multi-climate mode interactions drive hydrological and vegetation responses to hydroclimatic extremes in Australia. *Remote Sens. Environ.* **2019**, *231*, 111270. [\[CrossRef\]](#)
14. Peng, S.; Chen, A.; Xu, L.; Cao, C.; Fang, J.; Myneni, R.B.; E Pinzon, J.; Tucker, C.J.; Piao, S. Recent change of vegetation growth trend in China. *Environ. Res. Lett.* **2011**, *6*, 044027. [\[CrossRef\]](#)
15. Piao, S.; Wang, X.; Ciais, P.; Zhu, B.; Wang, T.; Liu, J. Changes in satellite-derived vegetation growth trend in temperate and boreal Eurasia from 1982 to 2006. *Glob. Chang. Biol.* **2011**, *17*, 3228–3239. [\[CrossRef\]](#)
16. Wang, X.; Piao, S.; Ciais, P.; Li, J.; Friedlingstein, P.; Koven, C.; Chen, A. Spring temperature change and its implication in the change of vegetation growth in North America from 1982 to 2006. *Proc. Natl. Acad. Sci. USA* **2011**, *108*, 1240–1245. [\[CrossRef\]](#)
17. Xu, L.; Myneni, R.B.; Iii, F.S.C.; Callaghan, T.V.; Pinzon, J.E.; Tucker, C.J.; Zhu, Z.; Bi, J.; Ciais, P.; Tømmervik, H.; et al. Temperature and vegetation seasonality diminishment over northern lands. *Nat. Clim. Chang.* **2013**, *3*, 581–586. [\[CrossRef\]](#)
18. Gazol, A.; Camarero, J.J.; Vicente-Serrano, S.M.; Sánchez-Salguero, R.; Gutiérrez, E.; De Luis, M.; Sangüesa-Barreda, G.; Novak, K.; Rozas, V.; Tiscar, P.A.; et al. Forest resilience to drought varies across biomes. *Glob. Chang. Biol.* **2018**, *24*, 2143–2158. [\[CrossRef\]](#)
19. Fang, W.; Huang, S.; Huang, Q.; Huang, G.; Wang, H.; Leng, G.; Wang, L.; Guo, Y. Probabilistic assessment of remote sensing-based terrestrial vegetation vulnerability to drought stress of the Loess Plateau in China. *Remote Sens. Environ.* **2019**, *232*, 111290. [\[CrossRef\]](#)
20. Niu, S.; Luo, Y.; Li, D.; Cao, S.; Xia, J.; Li, J.; Smith, M.D. Plant growth and mortality under climatic extremes: An overview. *Environ. Exp. Bot.* **2014**, *98*, 13–19. [\[CrossRef\]](#)
21. Zhao, A.; Zhang, A.; Liu, X.; Cao, S. Spatiotemporal changes of normalized difference vegetation index (NDVI) and response to climate extremes and ecological restoration in the Loess Plateau, China. *Theor. Appl. Clim.* **2018**, *132*, 555–567. [\[CrossRef\]](#)
22. Yu, C.; Huang, X.; Chen, H.; Huang, G.; Ni, S.; Wright, J.S.; Hall, J.; Ciais, P.; Zhang, J.; Xiao, Y.; et al. Assessing the Impacts of Extreme Agricultural Droughts in China Under Climate and Socioeconomic Changes. *Earth's Futur.* **2018**, *6*, 689–703. [\[CrossRef\]](#)
23. Xiao, L.; Liu, L.; Asseng, S.; Xia, Y.; Tang, L.; Liu, B.; Cao, W.; Zhu, Y. Estimating spring frost and its impact on yield across winter wheat in China. *Agric. For. Meteorol.* **2018**, *260*, 154–164. [\[CrossRef\]](#)
24. Li, P.; Zhu, D.; Wang, Y.; Liu, D. Elevation dependence of drought legacy effects on vegetation greenness over the Tibetan Plateau. *Agric. For. Meteorol.* **2020**, *295*, 108190. [\[CrossRef\]](#)

25. Didan, K.; Munoz, A.B.; Solano, R. *MODIS Vegetation Index User's Guide (MOD13 Series)*; Version 3.00 (Collection 6); University of Arizona: Tucson, AZ, USA, 2015.
26. Zheng, J.; Yin, Y.; Li, B. A New Scheme for Climate Regionalization in China. *Acta Geogr. Sin.* **2010**, *65*, 3–12. (In Chinese)
27. Alexander, L.; Herold, N. *ClimPACT2 Indices and Software*; The University of South Wales: Sydney, Australia, 2016; Available online: <https://github.com/ARCCSS-extremes/climpact2/> (accessed on 3 December 2020).
28. Tobler, W.R. A Computer Movie Simulating Urban Growth in the Detroit Region. *Econ. Geogr.* **1970**, *46*, 234. [[CrossRef](#)]
29. Brunsdon, C.; Fotheringham, A.S.; Charlton, M.E. Geographically Weighted Regression: A Method for Exploring Spatial Nonstationarity. *Geogr. Anal.* **2010**, *28*, 281–298. [[CrossRef](#)]
30. Fotheringham, A.S.; Charlton, M.; Brunsdon, C. The geography of parameter space: An investigation of spatial non-stationarity. *Int. J. Geogr. Inf. Syst.* **1996**, *10*, 605–627. [[CrossRef](#)]
31. Fotheringham, A.S.; Brunsdon, C.; Charlton, M. *Geographically Weighted Regression: The Analysis of Spatially Varying Relationships*; Wiley: Chichester, UK, 2002.
32. Fotheringham, A.S.; Oshan, T. GWR and Multicollinearity: Dispelling the myth. *J. Geogr. Syst.* **2016**, *18*, 303–329. [[CrossRef](#)]
33. Fotheringham, A.S.; Yang, W.; Kang, W. Multiscale Geographically Weighted Regression (MGWR). *Ann. Am. Assoc. Geogr.* **2017**, *107*, 1247–1265. [[CrossRef](#)]
34. Oshan, T.M.; Li, Z.; Kang, W.; Wolf, L.J.; Fotheringham, A.S. mgwr: A Python Implementation of Multiscale Geographically Weighted Regression for Investigating Process Spatial Heterogeneity and Scale. *ISPRS Int. J. Geo Inf.* **2019**, *8*, 269. [[CrossRef](#)]
35. Kohonen, T. *Self-Organizing and Associative Memory*; Springer: New York, NY, USA; Berlin/Heidelberg, Germany, 1988; ISBN 0-387-18314-0.
36. Zhang, F.; Wang, C.; Wang, Z.-H. Response of Natural Vegetation to Climate in Dryland Ecosystems: A Comparative Study between Xinjiang and Arizona. *Remote Sens.* **2020**, *12*, 3567. [[CrossRef](#)]
37. Abbas, S.; Nichol, J.E.; Wong, M.S. Trends in vegetation productivity related to climate change in China's Pearl River Delta. *PLoS ONE* **2021**, *16*, e0245467. [[CrossRef](#)]
38. Chu, H.; Venevsky, S.; Wu, C.; Wang, M. NDVI-based vegetation dynamics and its response to climate changes at Amur-Heilongjiang River Basin from 1982 to 2015. *Sci. Total. Environ.* **2019**, *650*, 2051–2062. [[CrossRef](#)]
39. Churkina, G.; Schimel, D.; Braswell, B.H.; Xiao, X. Spatial analysis of growing season length control over net ecosystem exchange. *Glob. Chang. Biol.* **2005**, *11*, 1777–1787. [[CrossRef](#)]
40. Gonsamo, A.; Chen, J.M.; Price, D.T.; Kurz, W.A.; Wu, C. Land surface phenology from optical satellite measurement and CO₂ eddy covariance technique. *J. Geophys. Res. Space Phys.* **2012**, *117*, 03032. [[CrossRef](#)]
41. Walther, S.; Voigt, M.; Thum, T.; Gonsamo, A.; Zhang, Y.; Koehler, P.; Jung, M.; Varlagin, A.; Guanter, L. Satellite chlorophyll fluorescence measurements reveal large-scale decoupling of photosynthesis and greenness dynamics in boreal evergreen forests. *Glob. Chang. Biol.* **2016**, *22*, 2979–2996. [[CrossRef](#)] [[PubMed](#)]
42. Krause, G.H.; Weis, E. Chlorophyll Fluorescence and Photosynthesis: The Basics. *Annu. Rev. Plant Biol.* **1991**, *42*, 313–349. [[CrossRef](#)]
43. Joiner, J.; Guanter, L.; Lindstrot, R.; Voigt, M.; Vasilkov, A.P.; Middleton, E.M.; Huemmrich, K.F.; Yoshida, Y.; Frankenberg, C. Global monitoring of terrestrial chlorophyll fluorescence from moderate-spectral-resolution near-infrared satellite measurements: Methodology, simulations, and application to GOME-2. *Atmos. Meas. Tech.* **2013**, *6*, 2803–2823. [[CrossRef](#)]
44. Frankenberg, C.; O'Dell, C.; Berry, J.; Guanter, L.; Joiner, J.; Köhler, P.; Pollock, R.; Taylor, T.E. Prospects for chlorophyll fluorescence remote sensing from the Orbiting Carbon Observatory-2. *Remote Sens. Environ.* **2014**, *147*, 1–12. [[CrossRef](#)]
45. Köhler, P.; Guanter, L.; Joiner, J. A linear method for the retrieval of sun-induced chlorophyll fluorescence from GOME-2 and SCIAMACHY data. *Atmos. Meas. Tech.* **2015**, *8*, 2589–2608. [[CrossRef](#)]
46. Sun, Y.; Frankenberg, C.; Wood, J.D.; Schimel, D.S.; Jung, M.; Guanter, L.; Drewry, D.T.; Verma, M.; Porcar-Castell, A.; Griffis, T.J.; et al. OCO-2 advances photosynthesis observation from space via solar-induced chlorophyll fluorescence. *Science* **2017**, *358*, eaam5747. [[CrossRef](#)] [[PubMed](#)]